JMEPEG (2010) 19:1264–1267
DOI: 10.1007/s11665-010-9634-0

1059-9495/$19.00

Investigation into Characteristics of Portevin-Le Chatelier Effect of an Al-Mg Alloy

Hassan Sheikh

(Submitted October 21, 2009; in revised form February 14, 2010)

In this study, the plastic instabilities associated with the Portevin-Le Chatelier (PLC) and their effects on the mechanical properties and the fracture surfaces have been investigated for AA 5083. Tensile tests were performed at various temperatures and strain rates in order to do so. Then, serrated and smooth yielding domains were determined in Ln $\dot{\varepsilon}$-1/T diagram. The stress-strain curves related to the serrated domain show the values of flow stress decreases by increasing the strain rate at a constant temperature. In addition, the plot of critical strain versus imposed strain rate indicates an inverse manner at very low strain rates. It is confirmed that the type of PLC bands alters the values of ductility. Also, scanning electron microscopy (SEM) was utilized to study the fracture surfaces of tensile test specimens. SEM images show that PLC effect or dynamic strain aging changes the fracture type and the feature of failure.

Keywords aluminum, mechanical testing, non-ferrous metals, Portevin-Le Chatelier

1. Introduction

Portevin-Le Chatelier (PLC) phenomenon (bands) or serrated yielding occurs in dilute alloys within a certain range of applied strain rates and temperatures. The domain of occurrence of this phenomenon is appropriately represented in Ln $\dot{\varepsilon}$-1/T diagram, where $\dot{\varepsilon}$ and T are the applied strain rate and the absolute temperature, respectively (Ref 1, 2). The phenomenon of DSA is the origin of these instabilities. At the nanoscale, DSA is explained by the dynamic interaction of mobile dislocations with the solute atoms (Ref 3). McCormick (Ref 4) and Van Den Beukel (Ref 5) demonstrated that the slip of mobile dislocations is discontinuous and that dislocations are temporarily stopped on the obstacles (such as forest dislocations and very fine precipitations) during a waiting time (t_w). Under working conditions, different types of bands may be created in stress-strain curves each of which alters the mechanical properties differently (Ref 6). The knowledge of PLC occurrence domain is very important; particularly, in sheet metal forming processes in which PLC phenomenon causes problems such stretcher-strain (st-st) marks on the surface and it must be prevented from applying conditions of PLC phenomenon occurrence (Ref 7). A significant feature of serrated flow curves in many aluminum alloys is the occurrence of an incubation strain before the onset of serrated yielding. The incubation period consisting of homogeneous plastic flow, is commonly referred to as critical strain (ε_c). This strain produces a critical concentration of vacancies, and the diffusion coefficient of the solute [responsible for dynamic strain aging (DSA) phenomenon] will enhance (Ref 6). The critical strain is observed to be influenced by both strain rate and temperature (Ref 8, 9). The value of ε_c increases by increasing the strain rate and by decreasing the temperature at high strain rates which is known as a normal manner. At high temperatures and low strain rates, an effect as an inverse manner can be observed for some alloys in which the value of ε_c increases by increasing the temperature or by decreasing the strain rate (Ref 6, 9).

To determine the suitable conditions of some metal forming processes such as sheet metal forming of AA 5083, the knowledge of the different metallurgical phenomena has a major contribution to eliminate the flow instabilities and strain localization. Therefore, the study of characteristics of DSA effect, PLC bands as a source of flow instabilities, and fracture types of AA 5083 is the prime objective of the present work.

2. Material and Experimental Procedure

The AA5083 slab with the initial thickness of 25 mm was used in this investigation. The composition of the employed material is given in Table 1. The as-received material was first annealed at 430 °C for 2 h and then air cooled. Figure 1 shows the microstructure of the material after the annealing process. Afterward, the tensile test specimens were machined out of the raw material. The geometry and dimensions of the specimens used in this study have been shown in Fig. 2. Laboratory tensile tests were carried out to assess the flow stress behavior as well as to study the PLC bands. The tensile tests were performed using an Instron machine, model 6027. It is worth noting that the crosshead speed during each experiment was kept constant; therefore, the true strain rate was being decreased slightly. Different average true strain rates were applied ranging between 10^{-4} and 10^{-1} (s^{-1}) and various temperatures were used from room temperature to 280 °C. To study the feature and the type of fracture in the tensile test specimens, two samples of the

Hassan Sheikh, Department of Materials Science and Engineering, Malek Ashtar University of Technology, P.O. Box 83145/115, Shahin Shahr, Iran and Department of Materials Science and Engineering, Sharif University of Technology, Azadi Ave., P.O. Box 11365-9466 Tehran, Iran. Contact e-mail: sheikh_scientific@yahoo.com.

Table 1 Chemical composition of the material used in this work (wt.%)

Element					
Mg	Mn	Si	Fe	Cr	Cu
4.5	0.71	0.33	0.19	0.058	0.037

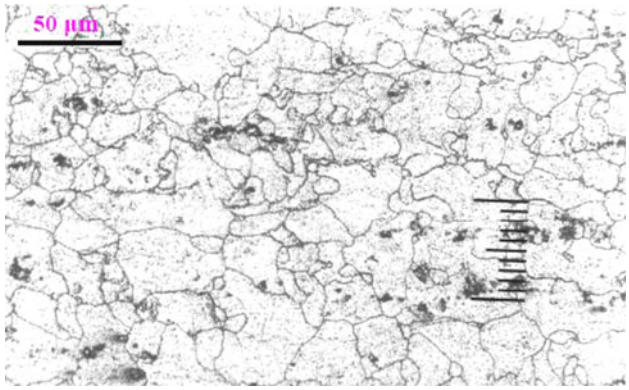

Fig. 1 Microstructure of the raw material after the annealing process

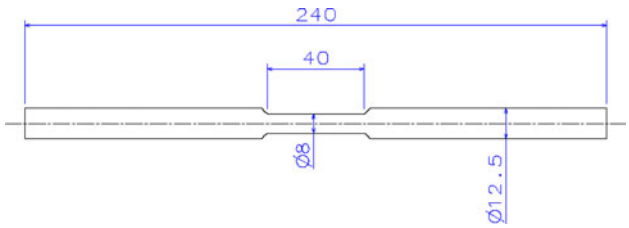

Fig. 2 The dimensions of the standard round tensile test specimen used in this study (dimensions in millimeter)

serrated and smooth yielding domains were selected, and SEM examinations were performed employing a PHILIPS XL 400.

3. Results and Discussion

Figure 3 shows true stress-strain curves under various temperatures and strain rates that DSA occurs under these working conditions. In this state, true stress-strain curves show negative strain rate sensitivity ($m = \partial \mathrm{Ln}\,\sigma / \partial \mathrm{Ln}\,\dot{\varepsilon} < 0$) and the value of flow stress decreases by increasing the applied strain rate at a constant temperature. It has been established that when a mobile dislocation reaches an obstacle, the magnesium atoms that are responsible for the occurrence of DSA in AA 5083, diffuse to the dislocation core and create a cluster which reduces the dislocation mobility. However, by increasing the applied strain rate, the creation of cluster around the core of dislocation is prevented due to the low value of t_w. As a result, the flow stress decreases (Ref 10). The variations of ultimate tensile strength (UTS) versus the applied temperature at the strain rates of 0.01 (s^{-1}) and 0.001 (s^{-1}) are shown in Fig. 4.

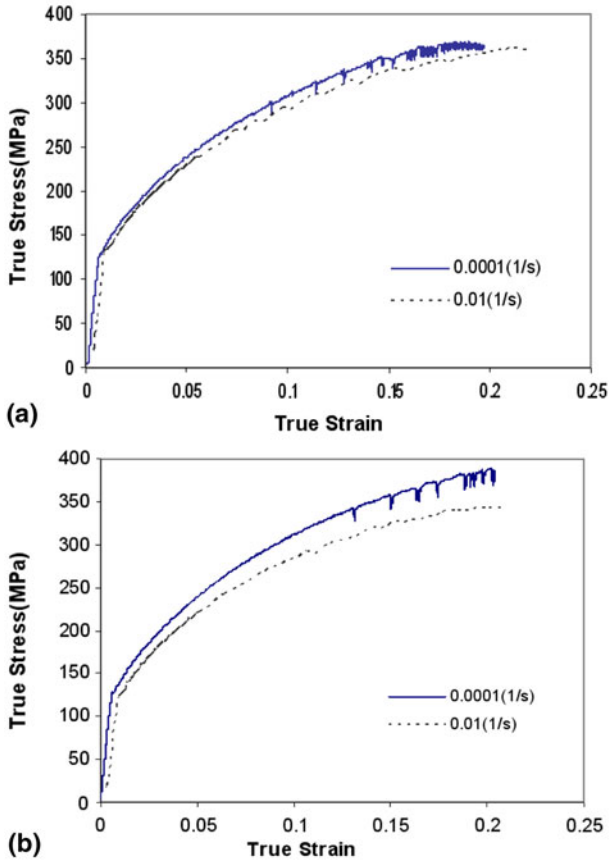

Fig. 3 True stress-strain curves achieved under different working conditions (a) at 25 °C and (b) at 86 °C

The lines drawn through the experimental points are based on the best-fit polynomial equations. Because of DSA phenomenon and the description mentioned above, the values of UTS decrease by increasing the strain rate at a constant temperature.

In Fig. 5, the domain of PLC instabilities was mapped in the log $\dot{\varepsilon}$-$1/T$ diagram using the stress-strain curves. Based on achieved stress-strain curves and using the Arrhenius-type equation as below (Ref 11), the activation energies of PLC boundary lines are "78 kJ/mol" and "15.1 kJ/mol" for the high- and low-temperature boundaries, respectively.

$$\dot{\varepsilon} = A \exp\left(-\frac{Q}{RT}\right), \qquad \text{(Eq 1)}$$

where A is a frequency factor, R is the gas constant, and Q is the activation energy of DSA occurrence. In the PLC domain and at a constant strain rate, it is easier for mobile dislocations to free from clusters of magnesium atoms by increasing the temperature. Therefore, the occurrence of DSA is difficult. For this reason, the activation energy of the high temperature PLC boundary line must be high. However at low temperatures, clusters easily lock mobile dislocations. Finally, the activation energy of the low-temperature PLC boundary line is very low.

In Fig. 6, nominal stress-strain curves at 25 °C and the types of PLC bands have been illustrated. The PLC band types have been termed A, B, C, and D each of which affects the mechanical properties differently. Type A bands propagate continuously and smoothly as solitary plastic waves and create

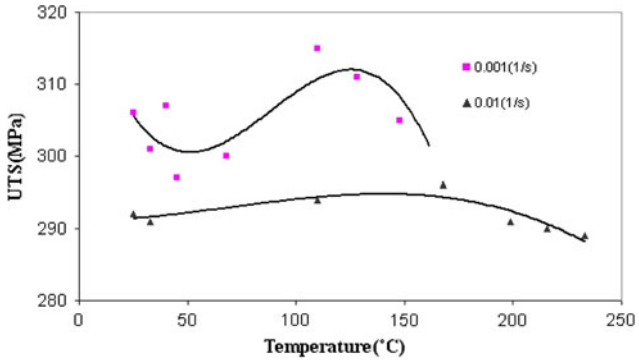

Fig. 4 Temperature dependence of the UTS at two strain rates

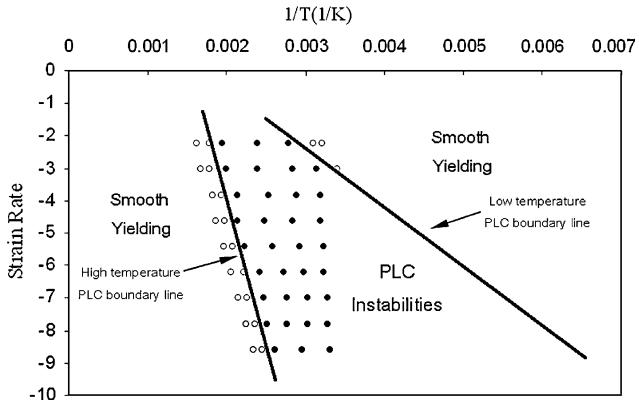

Fig. 5 Temperature and strain rate range in which PLC instabilities are observed

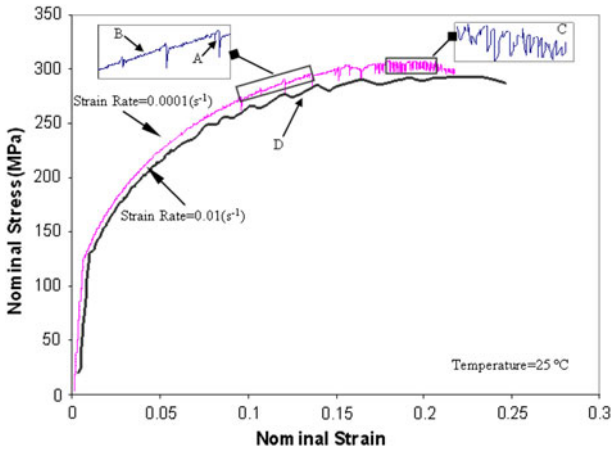

Fig. 6 Types of instabilities in nominal stress-strain curves at two working conditions

discontinuous points in stress-stress curves. These bands give rise to regular equidistant stress drops, and the value of stress drops is high. Type B bands exhibit an oscillatory or intermittent propagation along the tensile axis and their stress drops are very small (Ref 2, 12). The type C corresponds to the chaotic formation of the bands (discontinuous and not correlated) usually appearing in the end of stress-strain curve and

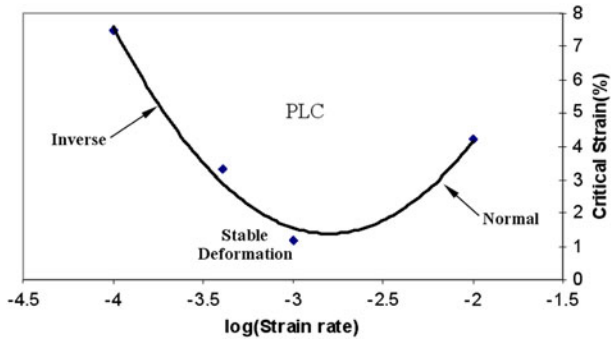

Fig. 7 The variation of critical strain vs. imposed strain rates at 25 °C

displaying an oscillation with medium stress drops. Type D bands are similar to type A bands, but the appearance of their stress drops are very continuous and smooth (Ref 6). By comparing stress-strain curves in Fig. 6, the effect of PLC band types on ductility values can be seen. It can be recognized that type C bands are a dominant type at the strain rate of 0.0001 (s^{-1}) and have a severe effect on decreasing the ductility. It can be attributed to their high frequency, the behavior of propagation (Ref 13), and relatively high stress drops. However, type D bands are seen at the strain rate of 0.01(s^{-1}). Due to their characteristics and low frequency, they have a negligible effect on decreasing the ductility.

The inverse manner of critical strain has been observed in several alloys, especially for Al-based alloy of the 5XXX series (Ref 8). In Fig. 7, critical strain versus imposed strain rates at 25 °C has been plotted. It is noteworthy that normal and inverse behaviors of the critical strain can be seen for AA 5083. In the normal domain, the critical strain increases by increasing the strain rate. Because the necessary time for diffusion of solute atoms and locking of mobile dislocations decreases. Therefore, it needs more strain for increasing the vacancies density and the occurrence of serrated yielding. However at very low strain rate ($\dot{\varepsilon} < 10^{-3}\ s^{-1}$), there is enough time for generation of Mg_2Al_3 precipitations and the number of effective solute magnesium atoms deteriorates by decreasing the strain. These conditions enhance the critical strain (Ref 9).

The results of SEM study on the fracture surfaces of tensile specimens with different types of yielding are shown in Fig. 8. It can be seen in Fig. 8(a) that the specimen with serrated yielding shows a dimple and cleavage facet indicating that the fracture is a mixed type. It can be attributed to DSA effect and PLC bands. For this specimen deformed at 25 °C, the voids initiate and grow until the strain reaches near the value of ε_{UTS}. In this moment, the intensity of DSA increases and the mobile dislocations move along a plane of maximum shear stress, and the process continues. Because the band in which the dislocations are moving effectively becomes softer than the surrounding material where the clustering of magnesium atoms is continuing in stationary dislocations (Ref 14), a localized deformation can occur at stresses lower than those required to activate slip on other planes. Finally, a catastrophic type of ductile failure occurs in localized shear bands in the direction of maximum shear stress at 45° to the tensile axis. As a result, the fracture of this specimen is a mixed type consisting of ductile and brittle fractures. On the other hand, the specimen with smooth yielding shows only a ductile dimple fracture (Fig. 8b).

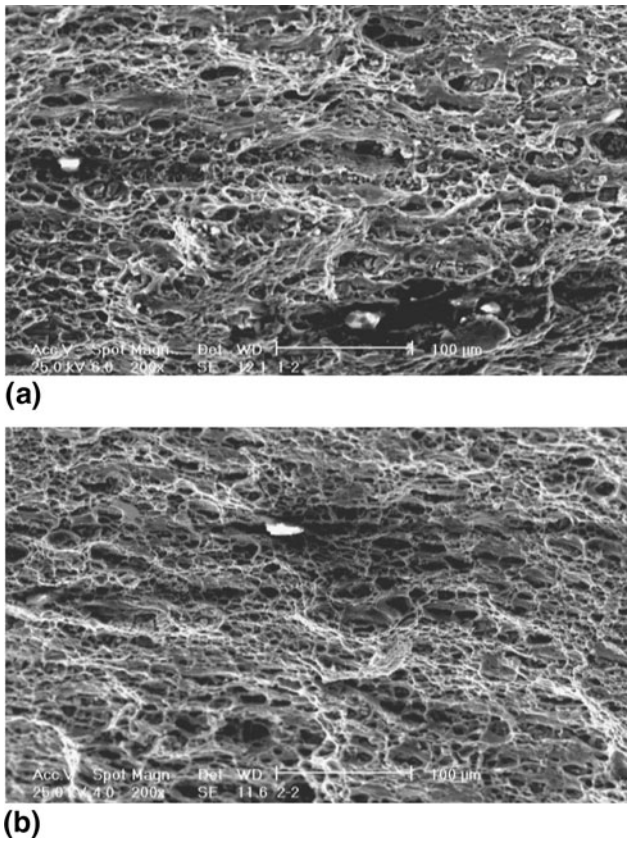

Fig. 8 SEM images of fracture surfaces for the samples with different types of yielding at the strain rate of 0.001 s^{-1}, (a) at 25 °C with serrated yielding and (b) at 168 °C with smooth yielding

For this specimen deformed at 168 °C, the voids initiate around the weakly bonded large precipitations of Mg_2Al_3 and other inclusions at early stage in the tensile test, and these start to grow until they finally link up by internal necking, producing classical ductile failure by microvoid coalescence (Ref 15, 16).

4. Conclusions

The characteristics of PLC instabilities and DSA effect, which are useful in practical applications such as sheet metal forming and rolling processes, were investigated in this work. The different types of PLC bands affect the values of the ductility. Under very low strain rates, the precipitations are created during tensile test and effective solute magnesium decreases. For this reason, an inverse manner of critical strain appeared in the plot of critical strain versus imposed strain rate. In addition, the mode of fracture changes with regard to PLC effect. This metallurgical aspect is susceptible to DSA phenomena imposing a shear-brittle mode of fracture surfaces.

Acknowledgments

The author thanks Sharif University of Technology. He appreciates Mr. Akhgar's help and support in the experimental work in mechanical properties laboratory.

References

1. R.C. Picu, G. Vincze, F. Ozturk, J.J. Gracio, F. Barlat, and A.M. Maniatty, Strain Rate Sensitivity of the Commercial Aluminum Alloy AA5182-O, *Mater. Sci. Eng. A*, 2005, **390**, p 334–343
2. M. Lebyodkin, L.D. Barkowskii, Y. Brechet, Y. Estrin, and L.P. Kubin, Spatio-Themporal Dynamics of the Portevin-Le Chatelier Effect, *Acta Mater.*, 2000, **48**, p 2529–2541
3. F.B. Klose, A. Ziegenbein, F. Hagemann, H. Neuhauser, P. Hahner, M. Abbadi, and A. Zeghloul, Analysis of Portevin-Le Chatelier Serrations of Type Bin Al-Mg, *Mater. Sci. Eng. A*, 2004, **369**, p 76–81
4. P.G. McCormick, The Portevin-Le Chatelier Effect in an Al-Mg-Si Alloy, *Acta Metal.*, 1971, **19**, p 463–471
5. A. Van Den Beukel, The Onset of Serrated Yielding in Au(Cu) Alloys, *Acta Metal.*, 1974, **22**, p 13–19
6. J.M. Robinson and M.P. Shaw, Microstructural and Mechanical Influences on Dynamic Strain Ageing Phenomena, *Int. Mater. Rev.*, 1994, **39**, p 113–121
7. T. Naka and F. Yoshida, Deep Drawability of Type 5083 Aluminum-Magnesium Alloy Sheet Under Various Conditions of Temperature and Forming Speed, *Mater. Proc. Tech.*, 1999, **89–90**, p 19–23
8. M. Abbadi, P. Hahner, and A. Zeghloul, On the Characteristics of Portevin-Le Chatelier Bands in Aluminum Alloy 5182 Under Stress-Controlled and Strain-Controlled Tensile Testing, *Mater. Sci. Eng. A*, 2002, **337**, p 194–201
9. K. Peng, W. Chen, and K. Quin, Study on Dynamic Strain Ageing Phenomenon of 3004 Aluminum Alloy, *Mater. Sci. Eng. A*, 2006, **415**, p 53–58
10. R.C. Picu and D. Zhang, Atomistic Study of Pipe Diffusion in Al-Mg Alloys, *Acta Mater.*, 2004, **5**, p 161–171
11. A. Karimi Taheri, T.M. Maccagno, and J.J. Jonas, Dynamic Strain Ageing and the Wire Drawing of Low Carbon Steel Rods, *ISIJ*, 1995, **35**, p 1532–1540
12. P. Hahner and E. Rizzi, On the Kinematics of Portevin-Le chatelier Bands, *Acta Mater.*, 2003, **51**, p 3385–3397
13. S. Liang, Z. Qing-Chung, and C. Peng-Tao, Influence of Solute Cloud and Precipitates on Spatiotemporal Characteristics of Portevin-Le Chatelier Effect in A2024 Aluminium Alloys, *Chin. Phys. B*, 2009, **18**, p 3500–3508
14. D. Zhang and R.C. Picu, Solute Clustering in Al-Mg Binary Alloys, *Model. Simulat. Mater. Sci. Eng.*, 2004, **12**, p 121–132
15. J.E. King, C.P. You, and J.F. Knott, Serrated Yielding and the Localized Shear Failure Mode in Aluminum Alloys, *Acta Metal.*, 1981, **29**, p 1553–1566
16. H. Karabulut and G. Suleiman, Effect of Vanadium Content on Dynamic Strain Ageing in Microalloyed Medium Carbon Steel, *Mater. Design*, 2004, **25**, p 521–527